

Promotion effects of acetoaceto-*o*-toluidide on *N*-butyl-*N*-(4-hydroxybutyl)nitrosamine-induced bladder carcinogenesis in rats

Nao Yukimatsu, Min Gi, Takahiro Okuno, Masaki Fujioka, Shugo Suzuki, Anna Kakehashi, Yukie Yanagiba, Megumi Suda, Shigeki Koda, Tatsuya Nakatani, Hideki Wanibuchi

Citation	Archives of Toxicology. 93(12); 3617–3631
Issue Date	2019-10-31
Type	Journal Article
Textversion	Author
Electronic supplementary material	Electronic supplementary material is available online at: https://doi.org/10.1007/s00204-019-02605-4 .
Right	This is a post-peer-review, pre-copyedit version of an article published in Archives of Toxicology. The final authenticated version is available online at: https://doi.org/10.1007/s00204-019-02605-4 . See Springer Nature terms of use. https://www.springer.com/gp/open-access/publication-policies/aam-terms-of-use .
DOI	10.1007/s00204-019-02605-4

Self-Archiving by Author(s)

Placed on: Osaka City University Repository

Promotion effects of acetoaceto-*o*-toluidide on *N*-butyl-*N*-(4-hydroxybutyl)nitrosamine-induced bladder carcinogenesis in rats

Nao Yukimatsu*‡, Min Gi*[·]#, Takahiro Okuno*, Masaki Fujioka*, Shugo Suzuki*, Anna Kakehashi*, Yukie Yanagiba§, Megumi Suda§, Shigeki Koda§, Tatsuya Nakatani‡, Hideki Wanibuchi*†

*Department of Molecular Pathology, Osaka City University Graduate School of Medicine, Osaka, Japan

#Present address: Department of Environmental Risk Assessment, Osaka City University Graduate School of Medicine, Osaka, Japan

‡Department of Urology, Osaka City University Graduate School of Medicine, Osaka, Japan

§Industrial Toxicology and Health Effects Research Group, National Institute of Occupational Safety and Health, Japan (JNIOSH), Kawasaki, Japan

†To whom correspondence should be addressed at: Osaka City University Graduate School of Medicine, Department of Molecular Pathology, Abeno-ku, 1-4-3 Asahi-machi,

Osaka, Japan; Tel: +81 6-6645-3735; Fax: +81 6-6646-3096; e-mail: wani@med.osaka-cu.ac.jp

Running Title: Promotion effects of AAOT on rat bladder carcinogenesis

Key words: AAOT, OTD, bladder carcinogenicity, rat, occupational urinary bladder cancer

Acknowledgments

This work was supported by a grant from Ministry of Health, Labor and Welfare, Japan, and Grant-in-Aid for Scientific Research from Japan Society for the Promotion of Science (JSPS KAKENHI Grant Number 18H06347 and 18K09146). We are grateful to Dr. Michiharu Matsumoto for his statistical consultant (Japan Bioassay Research Center, Japan Organization of Occupational Health and Safety). We gratefully acknowledge the technical assistance of Rie Onodera, Keiko Sakata, Yuko Hisabayashi, and Yukiko Iura (Department of Molecular Pathology, Osaka City University Graduate School of Medicine School), and Emi Donoue (Research Support Platform, Osaka City University Graduate School of Medicine).

Abstract

Recent epidemiological studies have indicated that occupational exposure to the aromatic amine acetoaceto-*o*-toluidide (AAOT) was associated with a marked increase in urinary bladder cancers in Japan. However, little is known about the carcinogenicity of AAOT. To evaluate the urinary bladder carcinogenicity of AAOT, male and female F344 rats were treated with *N*-butyl-*N*-(4-hydroxybutyl)nitrosamine (BBN) for 4 weeks followed by dietary administration of 0, 0.167, 0.5, or 1.5% AAOT for 31 weeks. The incidences and multiplicities of bladder tumors were significantly increased in the 0.5 and 1.5% groups of male and female rats in a dose-response manner. AAOT and 7 downstream metabolites were detected in the urine of the male and female rats administered AAOT with levels increasing in a dose-dependent manner. The most abundant urinary metabolite of AAOT was the human bladder carcinogen *o*-toluidine (OTD), which was at least one order of magnitude higher than AAOT and the other AAOT metabolites. In a second experiment, male F344 rats were administered 0, 0.167, or 1.5% AAOT for 4 weeks. Gene expression analyses revealed that expression of JUN and its downstream target genes were increased in the urothelium of male rats treated with 1.5% AAOT. These results demonstrate that AAOT promotes BBN-induced urinary bladder carcinogenesis in rats and suggest that overexpressed of JUN and its downstream target

genes may be involved the bladder carcinogenicity of AAOT. In conclusion, AAOT, like other carcinogenic aromatic amines, is likely to be a carcinogen to the urinary bladder, and OTD metabolized from AAOT is the ultimate carcinogen.

Introduction

Urinary bladder cancer is the fourth most common cancer and eighth most common cause of cancer death among men in the United States (Siegel et al. 2018). It is a significant cause of morbidity and mortality worldwide, with approximately 429,000 new cases resulting in 165,000 deaths annually (Ferlay et al. 2015). Smoking tobacco and occupational exposure to environmental carcinogens are considered the major risk factors for the development of urothelial carcinoma (Torre et al. 2015). A number of epidemiological and experimental studies have suggested that aromatic amines such as *o*-toluidine (OTD), 4-aminobiphenyl, benzidine, and 2-naphthylamine are associated with an increased risk of urinary bladder cancers (Cumberbatch et al. 2015; Ferris et al. 2013).

Acetoaceto-*o*-toluidide (AAOT) is a chemical substance used as an industrial intermediate in the synthesis of organic pigments (OECD 2003). From 2014 to 2017, ten workers in Japanese chemical plants engaged in the production of AAOT using OTD as a raw material were diagnosed with bladder cancer (Nakano et al. 2018). Because the workers were exposed to OTD and OTD is classified as a Group 1 carcinogen (“carcinogenic to humans”) by the International Agency for Research on Cancer (IARC 2012), OTD was considered to be the main cause of the urinary bladder cancers in these workers. However, the fact that the workers were also chronically exposed to AAOT

suggests the possibility that the occurrence of occupational urinary bladder cancers in these workers might be attributed to exposure to AAOT. In our previous 4-week short-term study, AAOT induced simple hyperplasia with increased cell proliferative activity and γ -H2AX expression, which is a novel marker for the prediction of potential carcinogenicity, in the bladder urothelium of male and female rats (Okuno et al. 2019). These findings suggested that AAOT is likely to be a bladder carcinogen. However, little is known about the mechanism of carcinogenicity of AAOT, and an understanding of the processes involved in AAOT carcinogenicity is indispensable for risk assessment of AAOT.

In the present study, we evaluated the effects of AAOT on rat urinary bladder carcinogenesis using a 36-week two-stage initiation-promotion carcinogenesis protocol. In a second experiment, to ascertain potential mechanisms of AAOT-mediated carcinogenicity, we used microarray gene expression analyses to investigate differential gene expression in the bladder urothelium of rats administered carcinogenic doses of AAOT for 4 weeks.

Materials and Methods

Chemicals and diets

N-Butyl-*N*-(4-hydroxybutyl)nitrosamine (BBN, purity > 98%), acetoaceto-*o*-toluidide (AAOT, purity > 98%), and *N*-acetyl-*o*-toluidine (*N*-acetyl-OTD, purity > 98%) were purchased from Tokyo Chemical Industry Co., Ltd. (Tokyo, Japan). *o*-toluidine (OTD, purity > 99%), 4-amino-*m*-cresol (4AMC, purity > 97%), 2-amino-*m*-cresol (2AMC, purity > 96%), 2-aminobenzyl alcohol (2ABA, purity > 98%), anthranilic acid (ATA, purity > 98%), and *N*-acetyl anthranilic acid (NAATA, purity > 98%) were purchased from Sigma-Aldrich Co., Ltd. (St. Louis, MO, USA). Acetonitrile (purity > 99.8%) and formic acid (purity > 98%) were purchased from Wako Pure Chemical Industries, Ltd. (Osaka, Japan). Basal diet (powdered MF) was purchased from Oriental Yeast Co., Ltd. (Tokyo, Japan) and diets containing AAOT were prepared once a month by Oriental Yeast Co., Ltd. (Tokyo, Japan).

Animals

Five-week-old male and female Fisher 344 rats were purchased from Charles River Laboratories Japan (Atsugi, Japan) and maintained in an animal facility with a

temperature of $22 \pm 3^{\circ}\text{C}$, a humidity of $55 \pm 5\%$, and a 12-h light/dark cycle. Rats were housed in plastic cages (3 rats/cage) with wood chips for bedding. Diet and tap water were available *ad libitum* throughout the study. Fresh diet was supplied to the animals twice weekly. They were observed daily for clinical signs and mortality. Body weight, food consumption, and water intake were measured weekly. The animals were acclimatized for one week prior to beginning the experiment. The animal experimental protocols were approved by The Laboratory Animal Center of Osaka City University Graduate School of Medicine, which is accredited by the Center for the Accreditation of Laboratory Animal Care and Use (CALAC), Japan Health Sciences Foundation (JHSF).

Experiment 1. Thirty-six-week two-stage urinary bladder carcinogenesis study

Experimental design

The experimental design is shown in Fig. 1. Eighty-one male rats and eighty-one female rats at six weeks of age were divided into 4 male and 4 female groups. All animals were given drinking water containing 0.05% BBN from the commencement of the experiment to week 4. One week after the end of BBN administration, rats were fed diets containing AAOT: 0 (control), 0.167, 0.5, or 1.5% AAOT for 31 weeks (from week 6 to 36). The highest dose of 1.5% was determined based on the results of our previous 4-

week study in which 1.5 and 3% AAOT promoted bladder epithelial cell proliferation and the 3% dose caused more than 20% suppression of body weight (Okuno et al. 2019). Fresh urine samples were collected by forced urination from rats in each group between 7:00 and 9:00 AM at week 36. All urine samples were centrifuged at 12000 rpm (13000 g) for 5 min and the supernatants were stored at -80°C. At the end of week 36, rats were euthanized by inhalation of an overdose of isoflurane (Abbott Japan Co., Ltd., Tokyo, Japan) using a Small Animal Anesthetizer (MK-A110D, Muromochi, Kikai Co., Ltd., Tokyo, Japan) coupled with an Anesthetic Gas Scavenging System (MK-T 100E, Muromochi Kikai Co., Ltd., Tokyo, Japan).

Pathological examination

At necropsy, urinary bladders were immediately inflated by injection of 4% phosphate-buffered paraformaldehyde (PFA) solution, and then fixed in the same PFA solution at 4°C for 4 hours. They were weighed, and relative organ weight was calculated using the final body weight. The location, number, and size of all suspected neoplastic lesions were recorded. Urinary bladders were then cut into eight strips and processed for embedding in paraffin. Paraffin-embedded tissue sections of urinary bladders were prepared for hematoxylin and eosin staining. Histopathological lesions of urinary bladder

epithelium were diagnosed as simple hyperplasia, papillary or nodular (PN) hyperplasia, papilloma, or urothelial carcinoma according to INHAND: International Harmonization of Nomenclature and Diagnostic Criteria for Lesions in Rats and Mice (Frazier et al. 2012).

Determination of the urinary metabolites of AAOT by LC-MS/MS analysis

LC-MS/MS analysis was performed on a Xevo TQD chromatographic system (Waters Co., Milford, MA, USA). The LC operating conditions were as follows: LC column, UK-Phenyl HT, 3 μm i.d., 2 mm \times 150 mm (Imtakt Co., Kyoto, Japan); 3 μl of the sample was injected using an autosampler (Sample Manager-FTN, Waters Co., Milford, MA, USA); the oven temperature was 35°C, and the total flow rate of the mobile phase was 0.4 mL/min. The analysis cycle for each sample was 10 min. The initial mobile phase composition, water/acetonitrile/25 mM formic acid (85/5/10), was maintained for 1 min. Acetonitrile was then added at a rate of 15%/min until it reached 75% and water was reduced to 15%, while 25 mM formic acid was held at 10%. The mobile phase composition of water, acetonitrile, and 25 mM formic acid at a ratio of 15:75:10 was maintained for 1.5 min. The mobile phase composition was then allowed to return to the initial conditions, followed by equilibration for 2.3 min, after which the next sample could

be loaded. The desolvation temperature was 600°C, and the desolvation gas flow was 1000 L/hr.

The MS/MS was operated with an electrospray ionization (ESI) source in the positive ion mode with multiple reaction monitoring (MRM). The nebulizer was set to a source temperature of 600°C and a gas flow rate of 1000 L/min. The capillary voltage was 0.5 kV (positive mode). High-purity nitrogen gas was used as the collision cell gas. The raw chromatograph and mass spectrogram data were processed with the MassLynx 4.1 software (Waters Co., Milford, MA, USA). The limit of detection (LOD) was 0.075 µM [AAOT], 0.17 µM [OTD], 0.0525 µM [*N*-acetyl-OTD], 0.98 µM [4AMC], 0.175 µM [2AMC], 0.295 µM [2ABA], 0.075 µM [ATA], and 0.595 µM [NAATA].

Experiment 2. Microarray gene expression analyses of urinary bladder epithelium of male rats administered AAOT for 4 weeks

Experimental design

Eighteen male rats at six weeks of age were randomly divided into 3 groups (6 rats in each group). Rats were fed diets containing AAOT: 0 (control), 0.167, or 1.5% for 4 weeks. Fresh urine samples were collected by forced urination from rats in each group between 7:00 and 9:00 AM at week 4. All urine samples were centrifuged at 12000 rpm

(13000 g) for 5 min and the supernatants were stored at -80°C as described in experiment 1. At the end of week 4, rats were euthanized by inhalation of an overdose of isoflurane as described in experiment 1. Methods used to collect rat bladder mucosa have been described previously (Wei et al. 2005). Briefly, urinary bladders were excised quickly and inverted on wooden applicator sticks. After rinsing with cold RNase free PBS buffer, bladder epithelial cells were removed by swirling the inverted bladders vigorously in microcentrifuge tubes containing RLT solutions supplied in the RNeasy Mini Kit (QIAGEN, Hilden, Germany). The solution containing the urinary bladder epithelial cells was kept on ice until RNA isolation; RNA isolation was performed within 2 hours of cell collection. Total RNAs were isolated using TRIZOL solution RNeasy Mini Kit according to the manufacturer's protocol.

Microarray gene expression analysis

A total of 6 µg of mRNA from the 6 rats of the control group and the 6 rats of the 1.5% group (1 µg each rat) were used for microarray analysis. Microarray analysis using a GeneChip® Rat Genome 230 2.0 Array (Affymetrix, Inc. Santa Clara, CA, USA) was performed by Cell Innovator Inc., Fukuoka, Japan. Briefly, cRNA was amplified, labeled using GeneChip WT PLUS Reagent Kit (Affymetrix, Inc. Santa Clara, CA, USA), and

hybridized to an Affymetrix Clariom D Assay Rat array, according to the manufacturer's instructions. All hybridized microarrays were scanned by an Affymetrix scanner. Relative hybridization intensities and background hybridization values were calculated using an Affymetrix Expression Console. Raw signal intensities for each probe were calculated from hybridization intensities. The raw signal intensities of samples from control and treated rats were \log_2 -transformed and normalized by SST-RMA and quantile algorithm (Bolstad et al. 2003) with Affymetrix Expression Console 1.1 software. To identify up or down-regulated genes, we calculated Z-scores (Quackenbush 2002) and ratios (non-log scaled fold-change) from the normalized signal intensities of each probe for comparison of samples from control and treated rats. Then we established criteria for regulated genes: (up-regulated genes) Z-score ≥ 2.0 and ratio ≥ 2.0 -fold, (down-regulated genes) Z-score ≤ -2.0 and ratio ≤ 0.5 . To investigate the functional significance of the up or down-regulated genes in the AAOT treatment groups, the list of differentially expressed genes was analyzed using Ingenuity Pathway Analysis (IPA) (Ingenuity Systems, Inc. Mountain View, CA, USA).

TaqMan real-time quantitative PCR

The mRNA expression levels of genes of interest genes were evaluated in 6 rats from

each group in experiment 2 by TaqMan real-time quantitative PCR. cDNA synthesis was performed with 1 µg of RNA using an Advantage RT-for-PCR kit (Takara Bio, Inc., Otsu, Japan). Primers and probes (Taqman Gene Expression Assay) for prostaglandin-endoperoxide synthase 2 (PTGS2) (also known as COX2), Jun proto-oncogene (JUN) (also known as c-JUN), plasminogen activator, urokinase (PLAU) (also known as uPA), early growth response 1 (EGR1), dual specificity phosphatase 1 (DUSP1) (also known as MKP1), tenascin C (TNC), serpin peptidase inhibitor, clade E member 1 (SERPINE1) (also known as PAI1), kinase insert domain receptor (KDR) (also known as VEGF Receptor 2), and matrix metalloproteinase 2 (MMP2) were purchased from Thermo Fisher Scientific, MA, USA. The real time RT-PCR assay was carried out with the Applied Biosystems 7500 Fast real-time PCR machine (Applied Biosystems, Inc., CA, USA). β -actin mRNA was employed as an internal control. Serially diluted standard cDNAs were included in each Taqman PCR reaction to create standard curves. The amounts of gene products in the test samples were estimated relative to the respective standard curve. Values for target genes were normalized to those for β -actin.

Determination of the urinary metabolites of AAOT by LC-MS/MS analysis

Determination of the urinary metabolites of AAOT by LC-MS/MS analysis was

performed as described in experiment 1.

Experiment 3. Immunohistochemical analysis of urinary bladders of male rats administered 1.5% AAOT for 4 weeks (Our previous 4-week experiment, (Okuno et al. 2019))

Immunohistochemical analysis

As urinary bladder specimens were used for microarray analysis of differential gene expression in experiment 2, paraffin-embedded urinary bladder specimens were not available; therefore, urinary bladder specimens from 6 rats per group from the control (0) and 1.5% AAOT male groups from our previous 4-week short-term toxicity study (Okuno et al. 2019) were used. Urinary bladder specimens were examined for expression of PTGS2 and JUN by immunohistochemical staining using the avidin-biotin-peroxidase complex (ABC) method. Paraffin sections (4- μ M thickness) were deparaffinized and dehydrated through a graded series of ethanol. Antigen retrieval was performed by microwaving at 98°C for 20 min in 0.01 M citrate buffer (pH 6.0). Endogenous peroxidase activity was blocked with 3% H₂O₂ in distilled water for 5 min. After blocking non-specific binding with goat serum at 37°C for 30 min, rat sections were incubated with mouse polyclonal anti-PTGS2 (COX2) antibody diluted 1:500 (610203, BD Bioscience,

California, USA) or rabbit monoclonal anti-JUN (c-JUN) antibody diluted 1:1000 (9165, Cell Signaling Technology, Danvers, USA) overnight at 4°C. Immunoreactivity was detected using VETASTAIN Elite ABC Kits for rabbit (Rabbit IgG, PK-6101, Vector Laboratories, Burlingame, USA) and mouse (Mouse IgG, PK-6102, Vector Laboratories, Burlingame, USA) primary antibodies and diaminobenzidin (DAB). To determine the percentage of JUN positive cells (JUN index), at least 3000 urothelial cells per rat in 6 rats from each group were counted using a light microscope.

Statistical analysis

All values were expressed as mean \pm standard deviation (SD). Statistical analyses were carried out with the GraphPad Prism version 7 program (GraphPad Software, San Diego, CA, USA). Homogeneity of variance was tested by the Bartlett's test (Experiment 1 and 2) or the F test (Experiment 3). In experiments 1 and 2, the differences in the mean values between the control and each treatment group were evaluated by the two-tailed Dunnett's multiple comparison test when the variance was homogeneous and by the two-tailed Dunn's multiple comparison test when variances were heterogeneous (multi-group comparisons). In the experiment 3, the variances were heterogeneous (two-group comparison), therefore, differences in the JUN-index were evaluated by the two-tailed

Welch's t-test. Trend analysis for incidences of histopathological lesions was conducted by the Chi-square test for trend (also known as the Cochran-Armitage trend test). Differences in the incidences of histopathological lesions in experiment 1 were compared using two-tailed Fisher's exact test. *P*-values less than 0.05 were considered statistically significant.

Results

Experiment 1: Thirty-six-week two-stage urinary bladder carcinogenesis study

General findings and urinary bladder weights

All animals survived until sacrifice. Final body weights, food and water consumption, AAOT intake, and urinary bladder weights are summarized in Table 1. The final body weights were significantly decreased in males in the 1.5% group and females in the 0.5 and 1.5% groups compared to their respective controls. The intake of AAOT was approximately proportional to the doses administered in the diet; although, average food consumption in the female 1.5% group tended to decrease compared to the control group. Average water intake was similar between the control and treated groups.

Absolute and relative urinary bladder weights were significantly increased in males in the 1.5% group and in females in the 0.5 and 1.5% groups in a dose-dependent manner. Absolute, but not relative urinary bladder weights, were significantly increased in males in the 0.5% group.

Macroscopic and histopathological observations in the urinary bladders

Macroscopically, larger urinary bladder tumors were most prevalent in the 0.5 and

1.5% male (Fig. 2a) and female (Fig. 2b) groups, and these likely contributed to the increased urinary bladder weights in these groups (Table 1). The incidence and multiplicity of PN hyperplasia, papillomas, carcinomas, and total tumors (papillomas and carcinomas) in the urinary bladder urothelium are summarized in Table 2. Trend tests showed a statistically significant correlation between AAOT dose and the incidence of PN hyperplasia, papillomas, carcinomas, and total tumors in male rats; and between AAOT dose and the incidence of PN hyperplasia, carcinomas, and total tumors in female rats. In male rats, the incidence of papillomas was significantly increased in the 1.5% group, and the incidence of carcinomas and total tumors were significantly increased in the 0.5 and 1.5% groups. The multiplicities of papillomas and carcinomas and total tumors were increased in the 1.5% group. In female rats, the incidence of carcinomas was significantly increased in the 0.5 and 1.5% groups, and the incidence of total tumors was increased in the 1.5% group. The multiplicities of the carcinomas and total tumors were significantly increased in the 0.5 and 1.5% groups. In addition, incidences and multiplicities of PN hyperplasia, a preneoplastic lesion in the rat urinary bladder (Cohen 2002), were significantly increased in males of the 0.167, 0.5, and 1.5% groups and in females of the 0.5 and 1.5% groups.

Metabolites of AAOT in the urine of rats

Urinary metabolites of AAOT at week 36 are shown in Table 3 and Fig. 6. AAOT and 7 downstream metabolites (OTD, *N*-acetyl-OTD, 4AMC, 2AMC, 2ABA, ATA, and NAATA) were detected in the male and female rats administered AAOT in a dose-dependent manner. Notably, OTD was the most abundant urinary metabolite and was at least one order of magnitude higher than AAOT and the other AAOT metabolites in the male and female rats. Unexpectedly, trace amounts of AAOT and OTD were detected in the urine of male and female control rats. Sources of environmental occurrence OTD include air, water, and food (IARC 2010). Therefore, while the exact reason why AAOT and OTD were detected in the control rats is unknown, one possible source is the basal diet. ATA was also detected in male and female control rats as it is a metabolite of the kynurenine metabolic pathway of diet-derived tryptophan (Friedman 2018; Michalowska et al. 2015).

Experiment 2: Microarray gene expression analyses of urinary bladder epithelium of male rats administered AAOT for 4 weeks

General findings

Final body weights, food and water consumption, and AAOT intake are summarized

in Table 1. The final body weights in the 1.5% AAOT group tended to decrease compared to the control group, albeit without statistical significance. The intake of AAOT was approximately proportional to the doses administered in the diet.

Metabolites of AAOT in the urine of rats

Urinary metabolites of AAOT in rats at week 4 are shown in Table 3. Similarly to the findings in the 36-week experiment (Experiment 1), the concentration of AAOT, OTD, and metabolites of OTD were increased in a dose-dependent manner in the male rats administered AAOT. OTD was the most abundant urinary metabolite and was at least one order of magnitude higher than AAOT and the other AAOT metabolites

Differentially expressed genes in the urothelium of male rats administered AAOT for 4 weeks by microarray gene expression analysis

A total of 94 genes, 65 overexpressed and 29 underexpressed genes, were differentially expressed in the urothelium of male rats administered 1.5% AAOT compared with the controls (Supplementary Table 1). Regulator Effects Analysis of the above 94 genes by IPA generated the “Growth of tumor” network shown in Fig. 3, including 2 upstream genes (JUN and PTGS2) and 7 downstream target genes (PLAU,

EGR1, DUSP1, TNC, SERPINE1, KDR, and MMP2).

Real-time Quantitative RT-PCR analysis

Relative mRNA expression of the 9 genes in the Growth of tumor network is shown in Fig. 4. Expression of the upstream genes JUN and PTGS2 and the downstream genes PLAU, DUSP1, and SERPINE1 were significantly increased in the urothelium of rats administered 1.5% AAOT. Expression of downstream genes EGR1, KDR, TNC, and MMP2 tended to be increased in the urothelium of rats administered 1.5% AAOT, albeit without statistical significance. While expression of the above 9 genes was not significantly increased by 0.167% AAOT, expression of all these genes tended to be increased compared to the control and show a dose-dependent response.

Experiment 3: Immunohistochemistry of JUN and PTGS2 in the urothelium of male rats administered 1.5% AAOT for 4 weeks (Our previous 4-week experiment, (Okuno et al. 2019))

As described in our previous study, simple hyperplasia of the urinary bladder epithelium was observed in 4/6 male rats in the 1.5% group, but PN hyperplasia was not observed in the 1.5% group (Okuno et al. 2019). Findings suggesting inflammation,

bleeding, or neutrophil infiltration were rarely observed, but some of the subepithelial stroma were slightly thickened, and fibroblasts and lymphocytes infiltrated the fibrous stroma in the 1.5% male group. In this study, representative immunohistochemical findings for JUN and PTGS2 in the urinary bladder are shown in Fig. 5. The JUN staining was observed within the nuclei of the urothelial cells in the control group (Fig. 5a1) and the morphologically normal urothelium (Fig. 5a2) and simple hyperplasia in the 1.5% group. The JUN index was significantly increased in the morphologically normal urothelium in the 1.5% group compared to the control group (Fig. 5a3). Positive PTGS2 staining was localized in the cytoplasm in the basal layer urothelial cells in the simple hyperplasia in the 1.5% group (Fig. 5b2) but was not present in normal urothelial cells in the controls (Fig. 5b1) or normal-like urothelial cells in the 1.5% group.

Discussion

AAOT is used for the synthesis of organic pigments and is made from OTD, which is a well-known human urinary bladder carcinogen (IARC 2012). However, little is known about the carcinogenicity of AAOT. In the present studies, we evaluated, for the first time, the modifying effects of AAOT on rat urinary bladder carcinogenesis, obtained detailed data on urinary metabolites of AAOT, and identified AAOT-induced gene expression alterations in the bladder urothelium. The results of the two-stage urinary bladder carcinogenesis study clearly demonstrated the promotion effects of AAOT on BBN-induced rat bladder carcinogenesis: 1) In male rats, the incidence of papillomas in the 1.5% group and the incidences of carcinomas and total tumors in the 0.5 and 1.5% groups were significantly increased compared to the control group. 2) In female rats, the incidence of carcinomas was significantly increased in the 0.5 and 1.5% groups, and the incidence of total tumors was increased in the 1.5% group. 3) The multiplicities of total tumors were significantly increased in the 0.5% female group and the 1.5% male and female groups. In addition, the findings of a statistically significant correlation between AAOT dose and the incidence of total tumors in male and female rats, the significantly increased incidences and multiplicities of PN hyperplasia, a preneoplastic lesion in the rat urinary bladder (Cohen 2002), in the 0.167% male group, and the markedly increased

urinary concentrations of OTD and its metabolites, strongly suggested that AAOT at the 0.167% level also promotes BBN-induced rat bladder carcinogenesis.

Urinary analyses of AAOT and its metabolites showed that AAOT and 7 downstream metabolites (OTD, *N*-acetyl-OTD, 4AMC, 2AMC, 2ABA, ATA, and NAATA) were increased in a dose-dependent manner in the urine of male and female rats administered AAOT. OTD was the most abundant urinary metabolite and was at least one order of magnitude higher than AAOT and the other AAOT metabolites in the urine of both male and female rats. This is consistent with the results of our previous study that AAOT, OTD, and *N*-acetyl-OTD were detected in the urine of male and female rats administered 3% AAOT for 3 days (Okuno et al. 2019). These findings indicated that AAOT was primarily converted into OTD and excreted into the urine, suggesting that OTD, a human bladder carcinogen (IARC 2012), metabolized from AAOT plays a pivotal role in the bladder carcinogenicity of AAOT. Furthermore, *N*-acetyl-OTD and 4AMC were detected in the urine of AAOT-treated rats, suggesting the existence of *N*-acetyl-4-amino-*m*-cresol, which is metabolite of *N*-acetyl-OTD and 4AMC (Fig. 6); although *N*-acetyl-4-amino-*m*-cresol was not measured due to the standard chemical not being commercially available. Notably, metabolism of *N*-acetyl-4-amino-*m*-cresol generates reactive oxygen species (ROS) and consequently induces urinary bladder epithelium cell proliferation (Dupont

1994; English et al. 2012).

While we did not evaluate the carcinogenic effects of AAOT alone because the amount of AAOT required for such a study is not commercially available, the facts that the major metabolite found in the urine in our studies was OTD, a bladder carcinogen in rats and humans (IARC 2012), and that carcinogenic metabolites of OTD, including *N*-acetyl-OTD, 4AMC, and 2AMC (Dupont 1994; Eitaki et al. 2019; English et al. 2012; Son et al. 1980) were also detected in the rats administered dietary AAOT, strongly suggest that OTD metabolized from AAOT plays a pivotal role in the carcinogenic effect of AAOT and suggest AAOT is likely to be a complete bladder carcinogen in rats and humans.

Gene expression and pathway analyses revealed that expression of JUN and its downstream target genes were upregulated in the urothelium of male rats treated with 1.5% AAOT for 4 weeks compared to the controls. JUN, a transcription factor in the activator protein-1 (AP-1) complex, is involved in numerous cell activities, such as proliferation, apoptosis, and differentiation (Bejjani et al. 2019; Shaulian and Karin 2002; Ye et al. 2014). Activation of JUN (AP-1) plays an important role in tumorigenesis, including urinary bladder cancers (Chen et al. 2012; Geng et al. 2017; Sun et al. 2017; Tiniakos et al. 1994; Zhao et al. 2018). As illustrated in the gene network “Growth of

tumor” (Fig. 3), JUN has been reported to directly induce expressions of PTGS2 (Chen et al. 2012; Grau et al. 2004), angiogenesis-related genes KDR (Wang et al. 2014) and DUSP1 (Kristiansen et al. 2010), and extracellular matrix-related genes MMP2 (Singh et al. 2010), SERPINE1 (Arts et al. 1999; Sundqvist et al. 2013), TNC (Arthur-Farraj et al. 2012), and PLAU (Herdegen and Leah 1998; Silberman et al. 1997). Moreover, overexpression of all 8 JUN-downstream genes PTGS2 (Agrawal et al. 2018; Czachorowski et al. 2012), KDR (Kopparapu et al. 2013), MMP2 (Peres et al. 2016), DUSP1 (Loda et al. 1996), EGR1 (Chen et al. 2017), SERPINE1 (Liu et al. 2016), TNC (di Martino et al. 2015; Guan et al. 2014), and PLAU (di Martino et al. 2015), have been reported in urinary bladder cancers. In our previous 4-week experiment, 1.5% AAOT also significantly increased cell proliferation activity in the urothelium (Okuno et al. 2019). Taken together, these results suggest that overexpression of JUN and its downstream target genes contributed, at least in part, to the induction of cell proliferation and the promotion effects of AAOT on BBN-induced bladder carcinogenesis.

PTGS2 (also known as COX-2) is an enzyme involved in the conversion of arachidonic acid to prostaglandin H₂ and is involved in tumor growth and is upregulated in urinary bladder cancer (Agrawal et al. 2018; Czachorowski et al. 2012). As illustrated in the gene network “Growth of tumor”, PTGS2 is directly induced by JUN (Chen et al.

2012; Grau et al. 2004) and indirectly induces expression of angiogenesis-related genes KDR (Garonna et al. 2011) and DUSP1 (Shah et al. 2014), the extracellular matrix-related gene MMP2 (Lau et al. 2010), and the transcription factor EGR1 (Diaz-Munoz et al. 2010). Furthermore, expression of JUN was significantly increased in the morphologically normal urothelium in rats administered 1.5% AAOT. In contrast, PTGS2 was negative in morphologically normal urothelium and increased in the simple hyperplasia in rats administered 1.5% AAOT. These findings suggest that overexpression of JUN was an early event and overexpression of PTGS2 occurred later, and provides indirect evidence that PTGS2 may be induced by JUN during AAOT-induced rat bladder carcinogenesis.

Based on the observations in the present experiments and the results from the literature (Dupont 1994; English et al. 2012; Son et al. 1980), metabolic pathways and potential modes of action for AAOT mediated rat urinary bladder carcinogenesis are shown in Fig. 6. OTD metabolized from AAOT is the key carcinogenic metabolite. *N*-hydroxyl-*o*-toluidine (*N*-hydroxyl-OTD) (not measured due to the standard chemical not being commercially available), a metabolite of OTD, binds covalently to DNA bases, which leads to DNA adduct formation in the bladder epithelium, causing DNA damage and mutagenicity (Bohm et al. 2011; Riedel et al. 2006). This is a well-established

carcinogenic mode of action for OTD. In another pathway, *N*-acetyl-OTD and 4AMC are metabolites of OTD, and *N*-acetyl-4-amino-*m*-cresol is a metabolite of *N*-acetyl-OTD and 4AMC, and *N*-acetyl-4-amino-*m*-cresol generates ROS, and ROS in turn can cause DNA and protein adduct formation that might contribute to the OTD-induced carcinogenesis (English et al. 2012; Son et al. 1980). Moreover, overexpression of JUN and its downstream target genes may also contribute to the carcinogenicity of AAOT. It has been suggested that ROS can activate JUN (Aggeli et al. 2006; Jackson and McArdle 2016). In addition, there is evidence that ROS generated by exposure to the aromatic amine 2-aminobiphenyl activates AP-1 (JUN) and subsequent PTGS2 expression in a human bladder cell line (Chen et al. 2012). Thus, metabolism of AAOT generates the metabolite *N*-hydroxyl-OTD that directly causes DNA damage and *N*-acetyl-4-amino-*m*-cresol that generate ROS that in turn causes protein and DNA damage and induces the overexpression of JUN and downstream target genes and subsequent cell proliferation, contributing to bladder carcinogenesis.

In conclusion, the results of the present studies demonstrate the promotion effects of AAOT on BBN-induced urinary bladder carcinogenesis in rats and suggest that overexpressed of JUN and its downstream target genes may be involved the bladder carcinogenicity of AAOT. Moreover, OTD metabolized from AAOT likely plays a pivotal

role in the carcinogenic effect of AAOT. In conclusion, our findings strongly indicate that AAOT, like other carcinogenic aromatic amines, is carcinogenic to the urinary bladder and that OTD metabolized from AAOT is the ultimate carcinogen of AAOT.

Ethical standards

The manuscript does not contain clinical studies or patient data.

Conflict of interest

The authors declare that they have no conflict of interest.

Reference

- Aggeli IK, Gaitanaki C, Beis I (2006) Involvement of JNKs and p38-MAPK/MSK1 pathways in H₂O₂-induced upregulation of heme oxygenase-1 mRNA in H9c2 cells. *Cell Signal* 18(10):1801-12 doi:10.1016/j.cellsig.2006.02.001
- Agrawal U, Kumari N, Vasudeva P, Mohanty NK, Saxena S (2018) Overexpression of COX2 indicates poor survival in urothelial bladder cancer. *Ann Diagn Pathol* 34:50-55 doi:10.1016/j.anndiagpath.2018.01.008
- Arthur-Farraj PJ, Latouche M, Wilton DK, et al. (2012) c-Jun reprograms Schwann cells of injured nerves to generate a repair cell essential for regeneration. *Neuron* 75(4):633-47 doi:10.1016/j.neuron.2012.06.021
- Arts J, Grimbergen J, Toet K, Kooistra T (1999) On the role of c-Jun in the induction of PAI-1 gene expression by phorbol ester, serum, and IL-1alpha in HepG2 cells. *Arterioscler Thromb Vasc Biol* 19(1):39-46
- Bejjani F, Evanno E, Zibara K, Piechaczyk M, Jariel-Encontre I (2019) The AP-1 transcriptional complex: Local switch or remote command? *Biochim Biophys Acta Rev Cancer* 1872(1):11-23 doi:10.1016/j.bbcan.2019.04.003
- Bohm F, Schmid D, Denzinger S, Wieland WF, Richter E (2011) DNA adducts of ortho-toluidine in human bladder. *Biomarkers* 16(2):120-8

doi:10.3109/1354750x.2010.534556

Bolstad BM, Irizarry RA, Astrand M, Speed TP (2003) A comparison of normalization methods for high density oligonucleotide array data based on variance and bias. *Bioinformatics* 19(2):185-93

Chen CC, Cheng YY, Chen SC, et al. (2012) Cyclooxygenase-2 expression is up-regulated by 2-aminobiphenyl in a ROS and MAPK-dependent signaling pathway in a bladder cancer cell line. *Chem Res Toxicol* 25(3):695-705
doi:10.1021/tx2004689

Chen J, Zhang N, Wen J, Zhang Z (2017) Silencing TAK1 alters gene expression signatures in bladder cancer cells. *Oncol Lett* 13(5):2975-2981
doi:10.3892/ol.2017.5819

Cohen SM (2002) Comparative pathology of proliferative lesions of the urinary bladder. *Toxicol Pathol* 30(6):663-71 doi:10.1080/01926230290166751

Cumberbatch MG, Cox A, Teare D, Catto JW (2015) Contemporary Occupational Carcinogen Exposure and Bladder Cancer: A Systematic Review and Meta-analysis. *JAMA Oncol* 1(9):1282-90 doi:10.1001/jamaoncol.2015.3209

Czachorowski MJ, Amaral AF, Montes-Moreno S, et al. (2012) Cyclooxygenase-2 expression in bladder cancer and patient prognosis: results from a large clinical

cohort and meta-analysis. PLoS One 7(9):e45025

doi:10.1371/journal.pone.0045025

di Martino E, Kelly G, Roulson JA, Knowles MA (2015) Alteration of cell-cell and cell-matrix adhesion in urothelial cells: an oncogenic mechanism for mutant FGFR3.

Mol Cancer Res 13(1):138-48 doi:10.1158/1541-7786.mcr-14-0022

Diaz-Munoz MD, Osma-Garcia IC, Cacheiro-Llaguno C, Fresno M, Iniguez MA (2010)

Coordinated up-regulation of cyclooxygenase-2 and microsomal prostaglandin E synthase 1 transcription by nuclear factor kappa B and early growth response-1 in macrophages. Cell Signal 22(10):1427-36 doi:10.1016/j.cellsig.2010.05.011

Dupont (1994) Urinary bladder toxicity-14-day feeding study with o-toluidine in rats.

Report DuPont HLR 699-93, OTS0557449

Eitaki Y, Nakano M, Kawai T, Omae K, Takebayashi T (2019) Biological monitoring of

o-toluidine in urine pretreated by an enzymatic deconjugation method. J Occup

Health 61(5):349-357 doi:10.1002/1348-9585.12058

English JC, Bhat VS, Ball GL, McLellan CJ (2012) Establishing a total allowable

concentration of o-toluidine in drinking water incorporating early lifestage exposure and susceptibility. Regul Toxicol Pharmacol 64(2):269-84

doi:10.1016/j.yrtph.2012.08.011

- Ferlay J, Soerjomataram I, Dikshit R, et al. (2015) Cancer incidence and mortality worldwide: sources, methods and major patterns in GLOBOCAN 2012. *Int J Cancer* 136(5):E359-86 doi:10.1002/ijc.29210
- Ferrís J, Garcia J, Berbel O, Ortega JA (2013) Constitutional and occupational risk factors associated with bladder cancer. *Actas Urol Esp* 37(8):513-22 doi:10.1016/j.acuro.2013.01.001
- Frazier KS, Seely JC, Hard GC, et al. (2012) Proliferative and nonproliferative lesions of the rat and mouse urinary system. *Toxicol Pathol* 40(4 Suppl):14s-86s doi:10.1177/0192623312438736
- Friedman M (2018) Analysis, Nutrition, and Health Benefits of Tryptophan. *Int J Tryptophan Res* 11:1178646918802282 doi:10.1177/1178646918802282
- Garonna E, Botham KM, Birdsey GM, Randi AM, Gonzalez-Perez RR, Wheeler-Jones CP (2011) Vascular endothelial growth factor receptor-2 couples cyclooxygenase-2 with pro-angiogenic actions of leptin on human endothelial cells. *PLoS One* 6(4):e18823 doi:10.1371/journal.pone.0018823
- Geng H, Zhao L, Liang Z, et al. (2017) Cigarette smoke extract-induced proliferation of normal human urothelial cells via the MAPK/AP-1 pathway. *Oncol Lett* 13(1):469-475 doi:10.3892/ol.2016.5407

- Grau R, Iniguez MA, Fresno M (2004) Inhibition of activator protein 1 activation, vascular endothelial growth factor, and cyclooxygenase-2 expression by 15-deoxy-Delta12,14-prostaglandin J2 in colon carcinoma cells: evidence for a redox-sensitive peroxisome proliferator-activated receptor-gamma-independent mechanism. *Cancer Res* 64(15):5162-71 doi:10.1158/0008-5472.can-04-0849
- Guan Z, Zeng J, Wang Z, et al. (2014) Urine tenascinC is an independent risk factor for bladder cancer patients. *Mol Med Rep* 9(3):961-6 doi:10.3892/mmr.2013.1873
- Herdegen T, Leah JD (1998) Inducible and constitutive transcription factors in the mammalian nervous system: control of gene expression by Jun, Fos and Krox, and CREB/ATF proteins. *Brain Res Brain Res Rev* 28(3):370-490
- IARC (2010) ortho-toluidine. IARC monographs on the evaluation of carcinogenic risks to humans. Vol 99, 407-469
- IARC (2012) ortho-toluidine. IARC monographs on the evaluation of carcinogenic risks to humans. Vol. 100F, 93-100
- Jackson MJ, McArdle A (2016) Role of reactive oxygen species in age-related neuromuscular deficits. *J Physiol* 594(8):1979-88 doi:10.1113/jp270564
- Kopparapu PK, Boorjian SA, Robinson BD, et al. (2013) Expression of VEGF and its receptors VEGFR1/VEGFR2 is associated with invasiveness of bladder cancer.

Anticancer Res 33(6):2381-90

Kristiansen M, Hughes R, Patel P, Jacques TS, Clark AR, Ham J (2010) Mkp1 is a c-Jun target gene that antagonizes JNK-dependent apoptosis in sympathetic neurons. *J Neurosci* 30(32):10820-32 doi:10.1523/jneurosci.2824-10.2010

Lau MT, Wong AS, Leung PC (2010) Gonadotropins induce tumor cell migration and invasion by increasing cyclooxygenases expression and prostaglandin E(2) production in human ovarian cancer cells. *Endocrinology* 151(7):2985-93 doi:10.1210/en.2009-1318

Liu M, Li M, Liu J, et al. (2016) Elevated urinary urea by high-protein diet could be one of the inducements of bladder disorders. *J Transl Med* 14:53 doi:10.1186/s12967-016-0809-9

Loda M, Capodieci P, Mishra R, et al. (1996) Expression of mitogen-activated protein kinase phosphatase-1 in the early phases of human epithelial carcinogenesis. *Am J Pathol* 149(5):1553-64

Michalowska M, Znorko B, Kaminski T, Oksztulska-Kolanek E, Pawlak D (2015) New insights into tryptophan and its metabolites in the regulation of bone metabolism. *J Physiol Pharmacol* 66(6):779-91

Nakano M, Omae K, Takebayashi T, Tanaka S, Koda S (2018) An epidemic of bladder

cancer: ten cases of bladder cancer in male Japanese workers exposed to ortho-toluidine. *J Occup Health* 60(4):307-311 doi:10.1539/joh.2017-0220-OA

OECD (2003) SIDS Initial Assessment Report for SIAM 16. o-Acetoacetotoluidide, CAS No: 93-68-5. URL: <https://hpvchemicals.oecd.org/UI/handler.axd?id=78eb2091-65d9-452d-94e1-74793f1366c8> Accessed 16 July 2019

Okuno T, Gi M, Fujioka M, et al. (2019) Acetoaceto-o-toluidide enhances cellular proliferative activity in the urinary bladder of rats. *Toxicol Sci* doi:10.1093/toxsci/kfz051

Peres R, Furuya H, Pagano I, Shimizu Y, Hokutan K, Rosser CJ (2016) Angiogenin contributes to bladder cancer tumorigenesis by DNMT3b-mediated MMP2 activation. *Oncotarget* 7(28):43109-43123 doi:10.18632/oncotarget.10097

Quackenbush J (2002) Microarray data normalization and transformation. *Nat Genet* 32 Suppl:496-501 doi:10.1038/ng1032

Riedel K, Scherer G, Engl J, Hagedorn HW, Tricker AR (2006) Determination of three carcinogenic aromatic amines in urine of smokers and nonsmokers. *J Anal Toxicol* 30(3):187-95

Shah S, King EM, Chandrasekhar A, Newton R (2014) Roles for the mitogen-activated protein kinase (MAPK) phosphatase, DUSP1, in feedback control of

- inflammatory gene expression and repression by dexamethasone. *J Biol Chem* 289(19):13667-79 doi:10.1074/jbc.M113.540799
- Shaulian E, Karin M (2002) AP-1 as a regulator of cell life and death. *Nat Cell Biol* 4(5):E131-6 doi:10.1038/ncb0502-e131
- Siegel RL, Miller KD, Jemal A (2018) Cancer statistics, 2018. *CA Cancer J Clin* 68(1):7-30 doi:10.3322/caac.21442
- Silberman S, Janulis M, Schultz RM (1997) Characterization of downstream Ras signals that induce alternative protease-dependent invasive phenotypes. *J Biol Chem* 272(9):5927-35
- Singh NK, Quyen DV, Kundumani-Sridharan V, Brooks PC, Rao GN (2010) AP-1 (Fra-1/c-Jun)-mediated induction of expression of matrix metalloproteinase-2 is required for 15S-hydroxyeicosatetraenoic acid-induced angiogenesis. *J Biol Chem* 285(22):16830-43 doi:10.1074/jbc.M110.106187
- Son OS, Everett DW, Fiala ES (1980) Metabolism of o-[methyl-14C]toluidine in the F344 rat. *Xenobiotica* 10(7-8):457-68
- Sun X, Deng Q, Liang Z, et al. (2017) Cigarette smoke extract induces epithelial-mesenchymal transition of human bladder cancer T24 cells through activation of ERK1/2 pathway. *Biomed Pharmacother* 86:457-465

doi:10.1016/j.biopha.2016.12.022

Sundqvist A, Zieba A, Vasilaki E, et al. (2013) Specific interactions between Smad proteins and AP-1 components determine TGFbeta-induced breast cancer cell invasion. *Oncogene* 32(31):3606-15 doi:10.1038/onc.2012.370

Tiniakos DG, Mellon K, Anderson JJ, Robinson MC, Neal DE, Horne CH (1994) c-jun oncogene expression in transitional cell carcinoma of the urinary bladder. *Br J Urol* 74(6):757-61

Torre LA, Bray F, Siegel RL, Ferlay J, Lortet-Tieulent J, Jemal A (2015) Global cancer statistics, 2012. *CA Cancer J Clin* 65(2):87-108 doi:10.3322/caac.21262

Wang W, Bian K, Vallabhaneni S, et al. (2014) ERK3 promotes endothelial cell functions by upregulating SRC-3/SP1-mediated VEGFR2 expression. *J Cell Physiol* 229(10):1529-37 doi:10.1002/jcp.24596

Wei M, Arnold L, Cano M, Cohen SM (2005) Effects of co-administration of antioxidants and arsenicals on the rat urinary bladder epithelium. *Toxicol Sci* 83(2):237-45 doi:10.1093/toxsci/kfi033

Ye N, Ding Y, Wild C, Shen Q, Zhou J (2014) Small molecule inhibitors targeting activator protein 1 (AP-1). *J Med Chem* 57(16):6930-48 doi:10.1021/jm5004733

Zhao L, Zhang T, Geng H, et al. (2018) MAPK/AP-1 pathway regulates benzidine-

induced cell proliferation through the control of cell cycle in human normal bladder epithelial cells. *Oncol Lett* 16(4):4628-4634 doi:10.3892/ol.2018.9155

Figure Captions

Figure 1

Experimental design of the 36-week two-stage urinary bladder carcinogenesis study (Experiment 1)

Fig.1

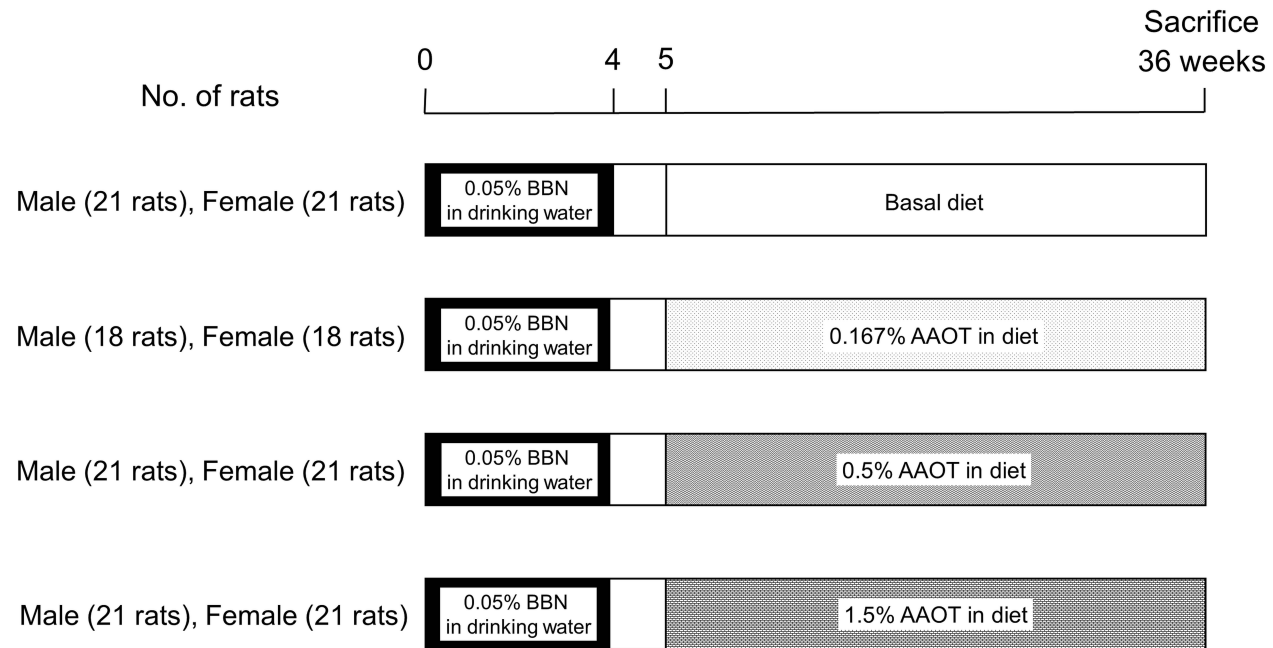


Figure 2

Macroscopic images of urinary bladders in experiment 1 (a: Male rat groups, b: Female rat groups). Urinary bladder tumors were increased in the 0.5 and 1.5% AAOT male and female groups compared with their respective control groups

Fig.2

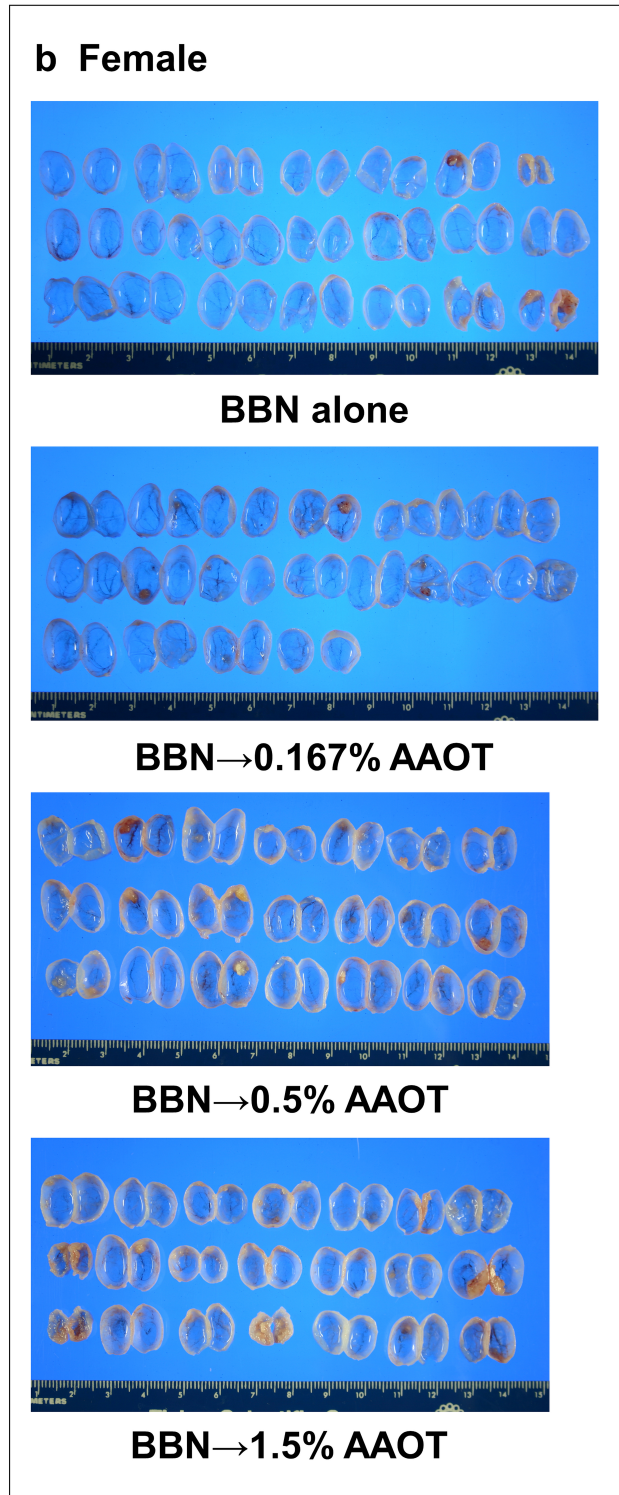
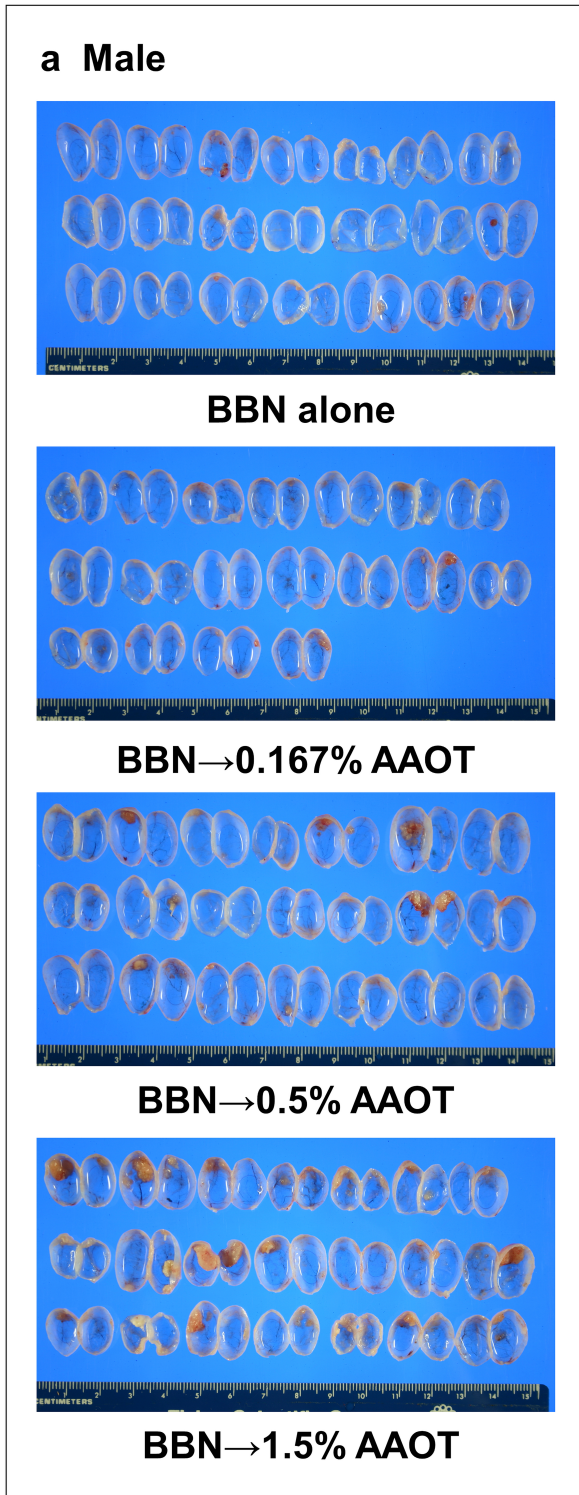


Figure 3

The “Growth of tumor” network identified by IPA in the male rats administered 1.5% AAOT for 4 weeks (Experiment 2). Lines and arrows represent direct (solid lines) and indirect (dashed lines) interactions between molecules

Fig.3

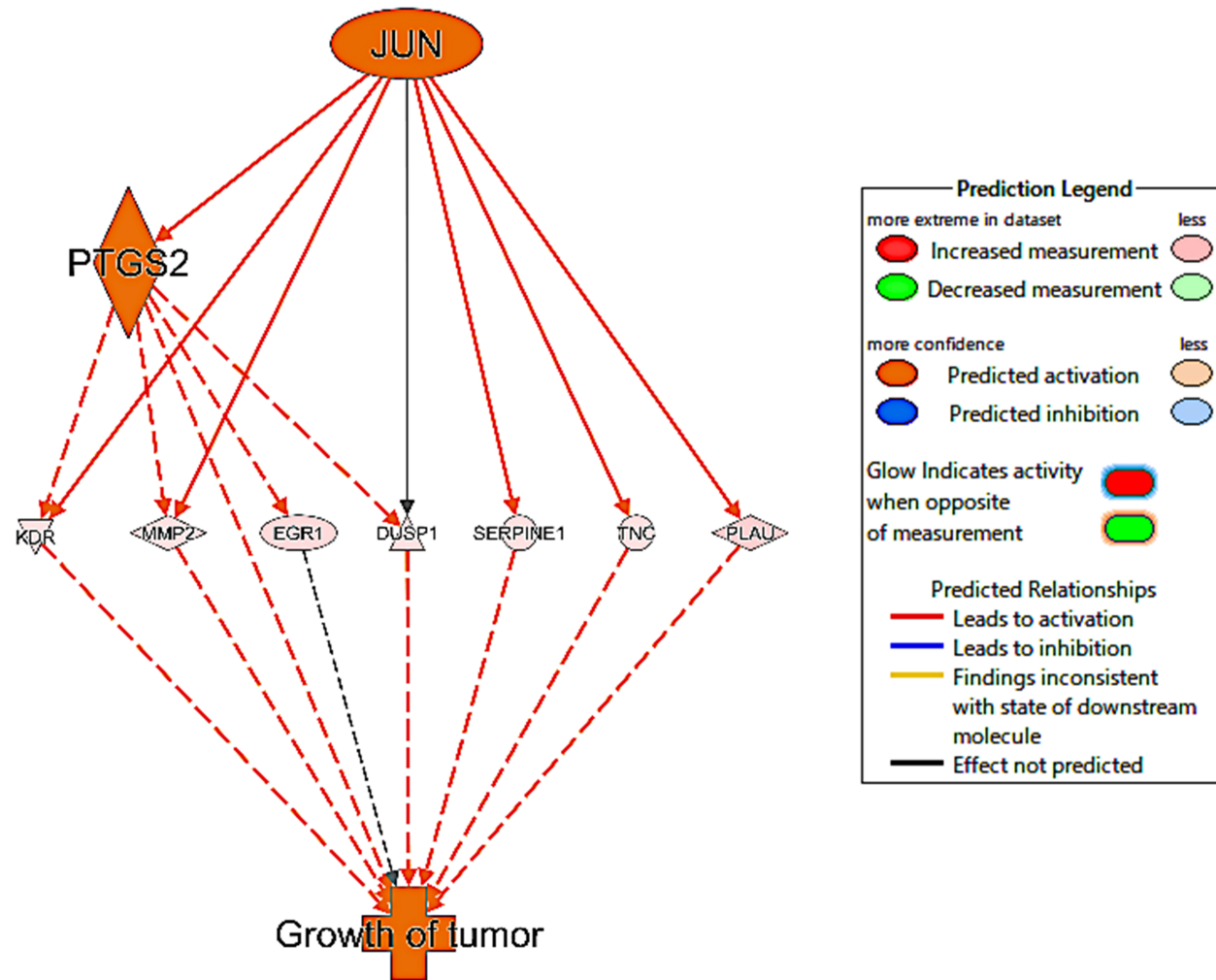


Figure 4

mRNA expression of PTGS2, JUN, PLA2, DUSP1, SERPINE1, EGR1, KDR, TNC, and MMP2 in the urothelium of 6 male rats from each group in the 4-week AAOT administration study (Experiment 2). Significant differences from the control group at * $p < 0.05$, ** $p < 0.01$, respectively

Fig.4

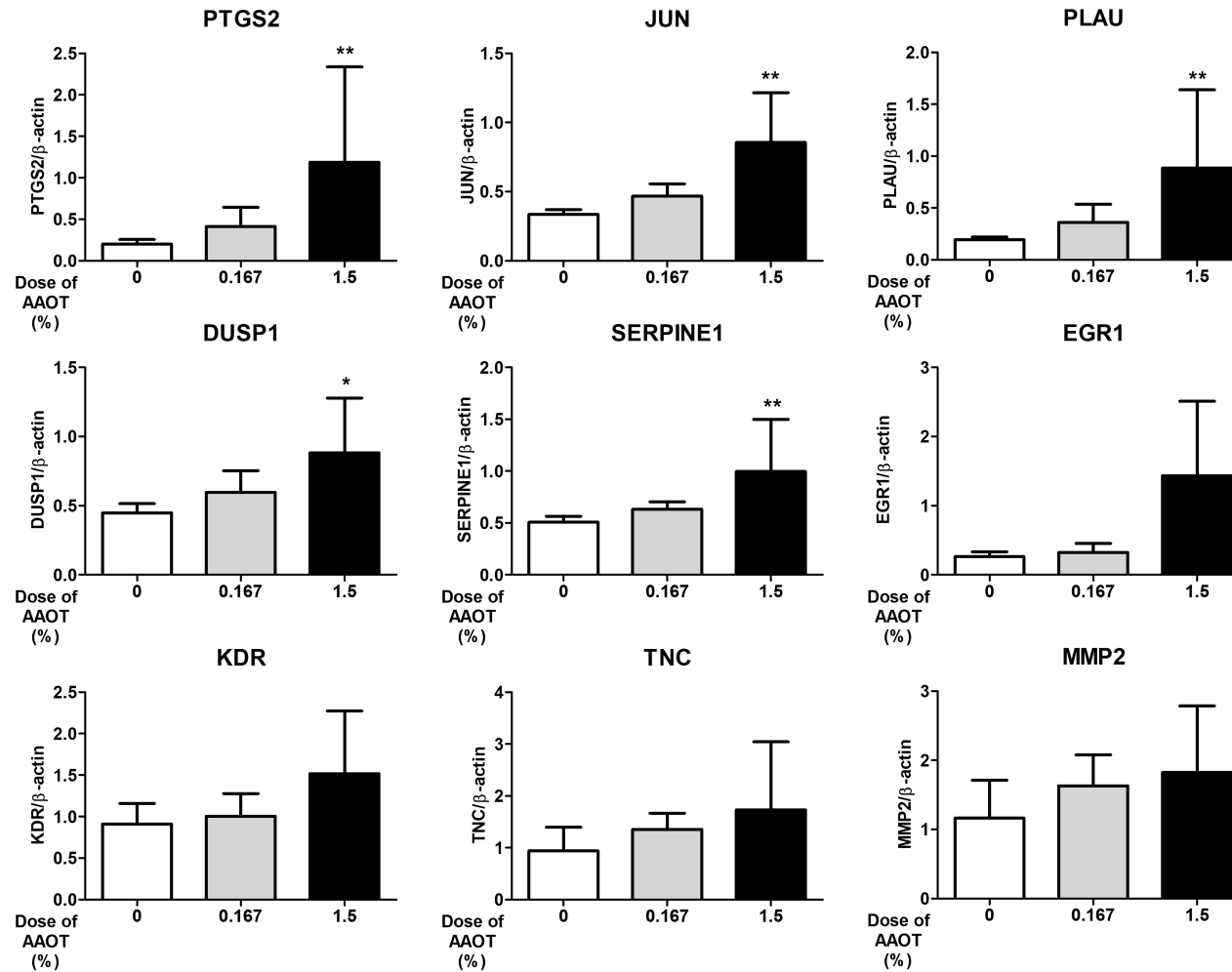


Figure 5

Immunohistochemistry of JUN (a) and PTGS2 (b) in the urothelium of male rats administered 1.5% AAOT for 4 weeks (Our previous 4-week experiment, (Okuno et al. 2019)). Positive JUN staining was localized within the nuclei of the urothelial cells: normal mucosa from a control rat (a1) and the morphologically normal appearing urothelium from an AAOT-treated rat (a2). The JUN index was significantly increased in the morphologically normal urothelium in the 1.5% group compared to the control group (a3). Increased expression of PTGS2 in AAOT-induced simple hyperplasia: positive PTGS2 staining was localized in cytoplasm in the basal layer urothelial cells in the simple hyperplasia in the 1.5% group (b2), but was not present in normal urothelial cells in the controls (b1). Bars = 50 μ m. Significant differences compared with the control group (* p <0.01)

Fig.5

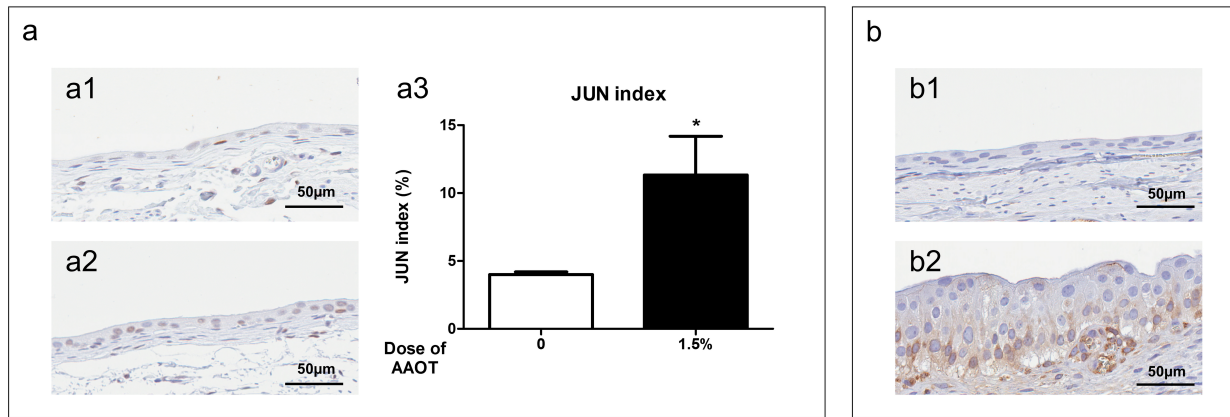


Figure 6

Metabolic pathway and potential modes of action for AAOT with regard to rat urinary bladder carcinogenesis. ↑; urinary concentration was increased in the AAOT-treated rats.

*; not measured due to the standard chemical not being commercially available. Findings reported in the present studies are highlighted in red.

Fig.6

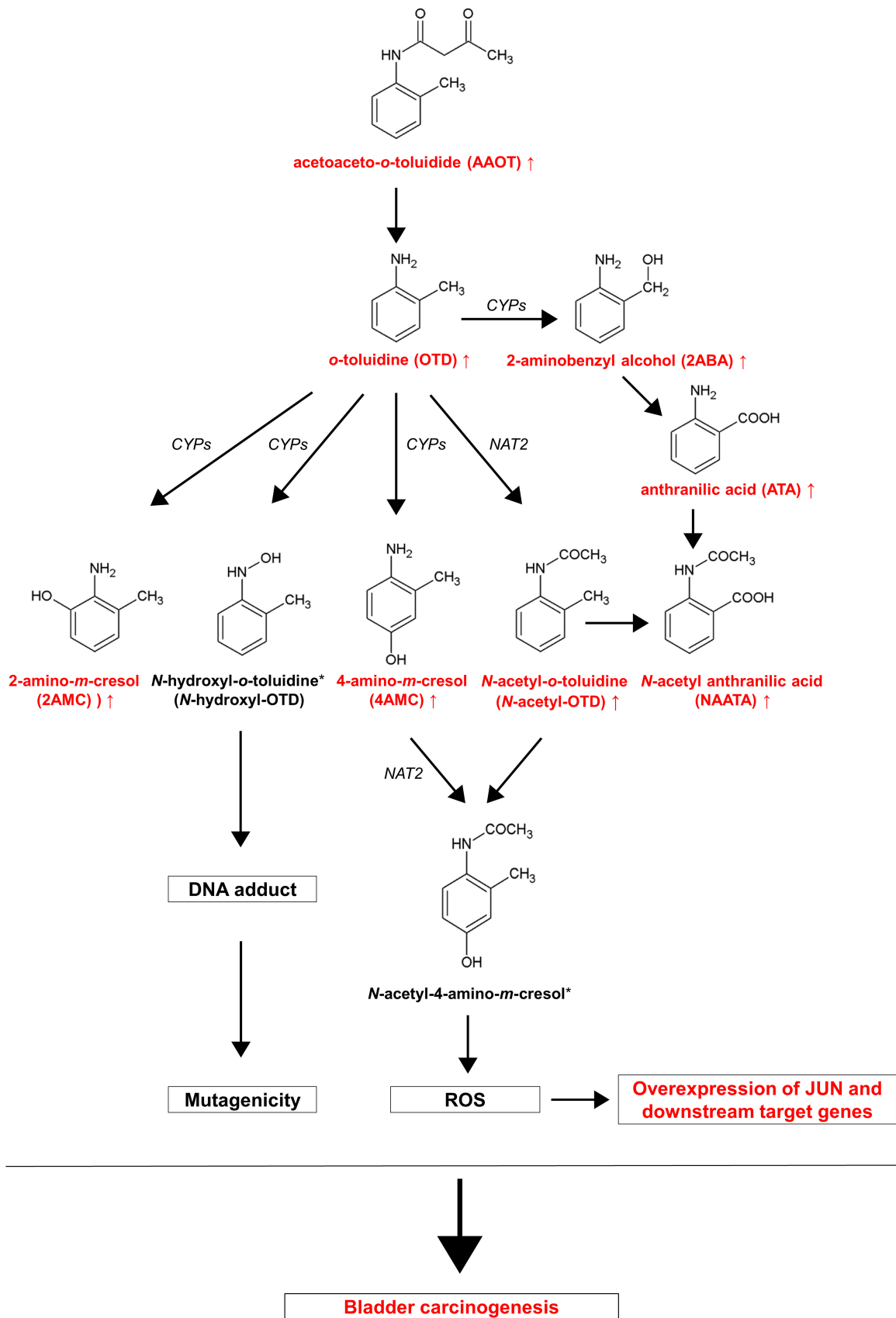


Table 1 Final body weights, food and water consumption, AAOT intake, and urinary bladder weights

Group	BBN	AAOT (%)	No. of rats	Final body weight (g)	Average food	Average water	Average intake	Urinary bladder weight	
					consumption (g/day/rat)	consumption (g/day/rat)	of AAOT (g/kg b.w./day)	Absolute (mg)	Relative (%)
Experiment 1 36-week two-stage urinary bladder carcinogenesis study									
Male									
	+	0	21	403.6 ± 19.5	14.0	19.4	0	139 ± 30	0.34 ± 0.08
	+	0.167	18	411.7 ± 19.1	14.0	19.8	0.07	153 ± 33	0.37 ± 0.09
	+	0.5	21	406.4 ± 14.1	14.2	19.8	0.21	171 ± 36*	0.42 ± 0.09
	+	1.5	21	364.4 ± 14.3**	14.1	19.2	0.65	239 ± 80**	0.66 ± 0.23**
Female									
	+	0	21	206.2 ± 8.3	9.1	14.6	0	108 ± 24	0.52 ± 0.12
	+	0.167	18	202.7 ± 8.2	9.2	15.4	0.08	122 ± 29	0.60 ± 0.15
	+	0.5	21	196.5 ± 6.5*	9.1	14.8	0.25	147 ± 36**	0.75 ± 0.19**
	+	1.5	21	185.8 ± 5.4**	8.4	14.6	0.71	161 ± 35**	0.87 ± 0.19**
Experiment 2 4-week AAOT administration study									
Male									
	—	0	6	233.4 ± 12.4	14.3	22.2	0		
	—	0.167	6	237.0 ± 13.8	14.7	21.9	0.12		
	—	1.5	6	221.9 ± 10.4	14.0	19.9	1.12		

Significant differences compared with the respective control group (*p<0.05, **p<0.01)

Table 2 Histopathological changes of the urinary bladder in 36-week two-stage urinary bladder carcinogenesis study (Experiment 1)

Group	BBN	AAOT (%)	No. of rats	Incidence (%)				Multiplicity			
				PN hyperplasia	Papillomas	Carcinomas	Total tumors (Papillomas + Carcinomas)	PN hyperplasia	Papillomas	Carcinomas	Total tumors (Papillomas + Carcinomas)
Male											
	+	0	21	14 (66.7%)	8 (38.1%)	3 (14.3%)	10 (47.6%)	1.1 ± 1.1	0.5 ± 0.7	0.1 ± 0.4	0.6 ± 0.7
	+	0.167	18	17 (94.4%)*	11 (61.1%)	4 (22.2%)	13 (72.2%)	2.7 ± 1.7*	0.7 ± 0.8	0.2 ± 0.4	0.9 ± 0.8
	+	0.5	21	21 (100%)**	14 (66.7%)	10 (47.6%)*	18 (85.7%)*	3.0 ± 1.6**	0.8 ± 0.7	0.6 ± 0.8	1.4 ± 1.0
	+	1.5	21	21 (100%)**	20 (95.2%)**	18 (85.7%)**	21 (100%)**	5.4 ± 3.0**	2.0 ± 1.2**	1.2 ± 0.9**	3.2 ± 1.5**
			Trend test	p<0.001	p<0.001	p<0.0001	p<0.0001				
Female											
	+	0	21	16 (76.2%)	5 (23.8%)	3 (14.3%)	7 (33.3%)	1.2 ± 0.9	0.2 ± 0.4	0.1 ± 0.4	0.4 ± 0.6
	+	0.167	18	16 (88.9%)	8 (44.4%)	5 (27.8%)	11 (61.1%)	2.3 ± 2.1	0.4 ± 0.5	0.3 ± 0.5	0.7 ± 0.7
	+	0.5	21	21 (100%)*	8 (38.1%)	10 (47.6%)*	14 (66.7%)	3.5 ± 2.5**	0.5 ± 0.7	0.5 ± 0.6*	1.0 ± 1.0*
	+	1.5	21	21 (100%)*	11 (52.4%)	11 (52.4%)*	17 (81.0%)**	4.7 ± 3.0**	0.9 ± 1.0	0.5 ± 0.5*	1.4 ± 1.1**
			Trend test	p<0.01	p=0.09	p<0.01	p<0.01				

Significant differences compared with the respective control group (*p<0.05, **p<0.01)

Table 3 Urinary metabolites in rats

Group	BBN	AAOT (%)	No. of rats	Urinary metabolites (μM)							
				AAOT ^a	OTD ^b	<i>N</i> -acetyl-OTD ^c	4AMC ^d	2AMC ^e	2ABA ^f	ATA ^g	NAATA ^h
Experiment 1	36-week two-stage urinary bladder carcinogenesis study										
Male											
	+	0	3	0.07 \pm 0.12	0.5 \pm 0.1	0	0	0	0	3.4 \pm 2.2	0
	+	0.167	3	2.67 \pm 0.29	69.6 \pm 38.3	9.0 \pm 2.0	1.2 \pm 0.2	1.2 \pm 0.2	0.7 \pm 0.5	10.3 \pm 6.3	1.4 \pm 0.1
	+	0.5	3	12.36 \pm 5.09	392.7 \pm 101.0	28.7 \pm 7.5	18.1 \pm 13.2	4.2 \pm 1.1	4.4 \pm 1.3	26.4 \pm 18.9	5.3 \pm 1.2
	+	1.5	3	57.62 \pm 37.68	3749.6 \pm 580.0	44.9 \pm 8.6	163.7 \pm 65.8	26.0 \pm 4.4	32.3 \pm 11.2	87.1 \pm 37.5	10.9 \pm 4.8
Female											
	+	0	5	0.02 \pm 0.05	0.3 \pm 0.2	0	0	0	0	0.5 \pm 0.1	0
	+	0.167	3	1.61 \pm 0.28	17.0 \pm 13.9	4.0 \pm 1.9	0.9 \pm 1.6	0.6 \pm 0.3	0.2 \pm 0.2	1.5 \pm 1.3	1.6 \pm 0.2
	+	0.5	3	4.53 \pm 1.14	106.8 \pm 22.4	26.5 \pm 6.0	13.5 \pm 11.7	1.3 \pm 0.5	1.8 \pm 0.7	2.4 \pm 2.4	5.0 \pm 0.5
	+	1.5	5	24.60 \pm 19.35	1191.1 \pm 674.0	39.1 \pm 15.5	78.9 \pm 45.8	26.2 \pm 7.1	10.3 \pm 3.8	10.7 \pm 10.1	20.8 \pm 7.4
Experiment 2	4-week AAOT administration study										
Male											
	—	0	3	0	0.1 \pm 0.1	0	0	0	0	8.7 \pm 4.0	0
	—	0.167	3	3.24 \pm 0.39	35.4 \pm 10.3	18.7 \pm 7.0	4.5 \pm 2.8	0.9 \pm 0.5	0.1 \pm 0.2	13.4 \pm 7.8	2.2 \pm 0.4
	—	1.5	3	57.60 \pm 30.14	4566.6 \pm 877.7	47.8 \pm 10.3	61.1 \pm 12.3	21.1 \pm 12.0	42.5 \pm 17.8	20.9 \pm 11.6	7.3 \pm 1.7

^a acetoaceto-*o*-toluidide, ^b *o*-toluidine, ^c *N*-acetyl-*o*-toluidine, ^d 4-amino-*m*-cresol, ^e 2-amino-*m*-cresol, ^f 2-aminobenzyl alcohol, ^g anthranilic acid, ^h *N*-acetyl anthranilic acid

Supplementary Table 1 List of differentially expressed genes in the urothelium of male rats administered 1.5% AAOT

ID	Gene symbol	Gene name	Expr Fold Change
NM_012940	CYP1B1	Cytochrome P450, family 1, subfamily B, polypeptide 1	29.274
NM_012540	CYP1A1	Cytochrome P450, family 1, subfamily A, polypeptide 1	25.198
NM_017232	PTGS2	Prostaglandin-endoperoxide synthase 2	14.123
NM_031972	ALDH3A1	Aldehyde dehydrogenase 3 family, member A1	11.774
NM_001113223	LOC100134871	Beta globin minor gene	9.684
NM_013085	PLAU	Plasminogen activator, urokinase	6.465
ENSRNOT00000048977	HBA2	Hemoglobin, alpha 2	6.232
NM_001013062	THBS1	Thrombospondin 1	5.775
NM_031327	CYR61	Cysteine-rich, angiogenic inducer, 61	5.704
NM_001024316	GATA5	GATA binding protein 5	5.307
NM_012551	EGR1	Early growth response 1	5.202
NM_021835	JUN	Jun proto-oncogene	4.86
NM_001024285	AHRR	Aryl-hydrocarbon receptor repressor	4.425
NM_001191815	ARHGAP28	Rho GTPase activating protein 28	4.013
ENSRNOT00000073858	FOXF1	Forkhead box F1	4
NM_206815	RNASE6	Ribonuclease, RNase A family, 6	3.998
mRNARGD7552624_1	ENTPD1	Etonucleoside triphosphate diphosphohydrolase 1	3.993
NM_013197	ALAS2	5-aminolevulinate synthase 2	3.801
NM_001108156	ITGA11	Integrin, alpha 11	3.727
NM_053352	ACKR3	Atypical chemokine receptor 3	3.625
NM_172067	SPON1	Spondin 1, extracellular matrix protein	3.558
NM_053313	F2RL2	Coagulation factor II (thrombin) receptor-like 2	3.309
NM_001004274	IGFBP4	Insulin-like growth factor binding protein 4	3.292
ENSRNOT00000043691	COL12A1	Collagen alpha-1 (XII) chain	3.113
NM_001106511	CPXM1	Carboxypeptidase X (M14 family), member 1	3.078
NM_001005562	CREB3L1	cAMP responsive element binding protein 3-like 1	3.076

Supplementary Table 1 (continued)

ID	Gene symbol	Gene name	Expr Fold Change
NM_001169138	THBS2	Thrombospondin 2	3.055
NM_001013853	HBA-A1	Hemoglobin alpha, adult chain 1	2.88
NM_181086	TNFRSF12A	Tumor necrosis factor receptor superfamily, member 12a	2.786
mRNARGD7640534_1	CNN2	Calponin 2	2.751
NM_001007002	MXRA8	Matrix-remodelling associated 8	2.703
NM_001007641	RND3	Rho family GTPase 3	2.703
ENSRNOT00000002790	BOC	BOC cell adhesion associated, oncogene regulated	2.604
NM_001271362	SCUBE3	Signal peptide, CUB domain, EGF-like 3	2.597
NM_053769	DUSP1	Dual specificity phosphatase 1	2.547
NM_133575	IL1RL2	Interleukin 1 receptor-like 2	2.534
NM_001191840	TGFB11	Transforming growth factor beta 1 induced transcript 1	2.515
NM_053861	TNC	Tenascin C	2.486
NM_012620	SERPINE1	Serpin peptidase inhibitor, clade E , member 1	2.458
NM_012760	PLAGL1	Pleiomorphic adenoma gene-like 1	2.423
mRNARGD2338799_1	GSTA2	Glutathione S-transferase alpha 2	2.414
NM_022605	HPSE	Heparanase	2.381
NM_053802	TGFBI	Transforming growth factor, beta induced	2.369
NM_001191770	PLEKHH2	Pleckstrin homology domain containing, family H, member 2	2.299
ENSRNOT00000015466	SCP2	Sterol carrier protein 2	2.259
NM_012827	BMP4	Bone morphogenetic protein 4	2.257
NM_001108168	BMP5	Bone morphogenetic protein 5	2.203
NM_017180	PHLDA1	Pleckstrin homology-like domain, family A, member 1	2.202
NM_001013137	CXCL14	Chemokine (C-X-C motif) ligand 14	2.198
NM_022266	CTGF	Connective tissue growth factor	2.154
NM_134329	ADH7	Alcohol dehydrogenase 7 (class IV), mu or sigma polypeptide	2.141
ENSRNOT00000015387	TIPARP	TCDD-inducible poly (ADP-ribose) polymerase	2.116

Supplementary Table 1 (continued)

ID	Gene symbol	Gene name	Expr Fold Change
NM_001270713	BDKRB2	Bradykinin receptor B2	2.113
NM_017123	AREG	Amphiregulin	2.107
NM_031560	CTSK	Cathepsin K	2.081
NM_012802	PDGFRA	Platelet derived growth factor receptor, alpha polypeptide	2.062
NM_013062	KDR	Kinase insert domain receptor	2.056
Col6a3.aSep08	COL6A3	Collagen, type VI, alpha 3	2.054
NM_031825	FBN1	Fibrillin 1	2.054
NM_031721	HTRA1	HtrA serine peptidase 1	2.038
NM_133608	SLCO4A1	Solute carrier organic anion transporter family, member 4a1	2.032
NM_031054	MMP2	Matrix metalloproteinase 2	2.021
NM_001008694	RCN3	Reticulocalbin 3, EF-hand calcium binding domain	2.019
NM_012950	F2R	Coagulation factor II (thrombin) receptor	2.017
NM_053304	COL1A1	Collagen, type I, alpha 1	2.011
ENSRNOT00000014460	NFE2L3	Protein Nfe2l3	-2.002
NM_057099	PSMB6	Proteasome subunit beta 6	-2.063
NM_031109	RPS10	Ribosomal protein S10	-2.072
NM_173128	KRT20	Keratin 20, type I	-2.108
NM_012618	S100A4	S100 calcium-binding protein A4	-2.135
NM_133526	TSPAN8	Tetraspanin 8	-2.177
NM_021770	OLIG1	Oligodendrocyte transcription factor 1	-2.203
NM_138843	MPST	Mercaptopyruvate sulfurtransferase	-2.21
NM_012488	A2M	Alpha-2-macroglobulin	-2.262
NM_145782	CYP3A18	Cytochrome P450, family 3, subfamily a, polypeptide 18	-2.269
NM_001191953	PGM5	Phosphoglucomutase 5	-2.295
NM_001106917	PI15	Peptidase inhibitor 15	-2.352
NM_012893	ACTG2	Actin, gamma 2, smooth muscle, enteric	-2.359

Supplementary Table 1 (continued)

ID	Gene symbol	Gene name	Expr Fold Change
NM_017348	SLC6A8	Solute carrier family 6 (neurotransmitter transporter), member 8	-2.598
mRNARGD2341490_t01	RGD1562378	Histone H4 variant H4-v.1	-2.631
NM_001170600	MYH11	Myosin, heavy chain 11, smooth muscle	-2.668
mRNARGD7529416_1	LOC102551184	Histone H4-like	-2.673
ENSRNOT00000071690	HIST2H4A	Histone H4 osteogenic growth peptide	-2.684
ENSRNOT00000074526	HIST1H4B	Histone cluster 1, H4b	-2.684
NM_001142367	P2RX1	Purinergic receptor P2X, ligand-gated ion channel, 1	-2.685
NM_139252	PLPP2	Phospholipid phosphatase 2	-2.757
NM_022280	LRAT	Lecithin-retinol acyltransferase	-2.809
NM_001191963	SYNPO2	Synaptopodin 2	-2.847
NM_207593	PSBPC2	Prostatic steroid-binding protein C2	-2.947
NM_133285	HIST1H1D	Histone cluster 1, H1d	-3.02
NM_022531	DES	Desmin	-3.797
mRNARGD2652116_1	PCP4	Purkinje cell protein 4	-4.387
NM_012718	ANDPRO	Androgen regulated protein	-11.693
NM_080770	SCGB2A2	Secretoglobin, family 2A, member 1	-17.317